ENVIRONMENTAL RESEARCH
LETTERS

OPEN ACCESS

RECEIVED
22 February 2021

REVISED
2 August 2021

ACCEPTED FOR PUBLICATION
6 August 2021

PUBLISHED
9 September 2021

LETTER

Late twentieth century rapid increase in high Asian seasonal snow and glacier-derived streamflow tracked by tree rings of the upper Indus River basin

Feng Chen[1,2,*], Magdalena Opała-Owczarek[3], Adam Khan[4], Heli Zhang[2], Piotr Owczarek[5], Youping Chen[1], Moinuddin Ahmed[6] and Fahu Chen[7,8]

[1] Yunnan Key Laboratory of International Rivers and Transboundary Eco-Security, Institute of International Rivers and Eco-Security, Yunnan University, Kunming, People's Republic of China
[2] Key Laboratory of Tree-ring Physical and Chemical Research of China Meteorological Administration/Xinjiang Laboratory of Tree-Ring Ecology, Institute of Desert Meteorology, China Meteorological Administration, Urumqi 830002, People's Republic of China
[3] Institute of Earth Sciences, Faculty of Natural Sciences, University of Silesia in Katowice, Ul. Bedzinska 60, Sosnowiec 41-200, Poland
[4] Department of Biological Science, University of Lakki Marwat KP, Pakistan
[5] Institute of Geography and Regional Development, University of Wroclaw, Pl.Uniwersytecki 1, Wrocław 50-137, Poland
[6] Research Laboratory of Dendrochronology and Plant Ecology, Department of Botany, Federal Urdu University of Arts, Science and Technology, Karachi, Pakistan
[7] Key Laboratory of Alpine Ecology, CAS Center for Excellence in T ibetan Plateau Earth Sciences and Institute of Tibetan Plateau Research, Chinese Academy of Sciences (CAS), Beijing 100101, People's Republic of China
[8] Key Laboratory of Western China's Environmental Systems (Ministry of Education), College of Earth and Environmental Sciences, Lanzhou University, Lanzhou, People's Republic of China
[*] Author to whom any correspondence should be addressed.

E-mail: feng653@163.com

Keywords: upper Indus River, high Asia, tree rings, streamflow reconstruction, volcanic eruption, solar activity

Abstract

Given the reported increasing trends in high Asian streamflow and rapidly increasing water demand in the Indian subcontinent, it is necessary to understand the long-term changes and mechanisms of snow- and glacier-melt-driven streamflow in this area. Thus, we have developed a June–July streamflow reconstruction for the upper Indus River watershed located in northern Pakistan. This reconstruction used a temperature-sensitive tree-ring width chronology of *Pinus wallichiana*, and explained 40.9% of the actual June–July streamflow variance during the common period 1970–2008. The high level of streamflow (1990–2017) exceeds that of any other time and is concurrent with the impact of recent climate warming that has resulted in accelerated glacier retreats across high Asia. The streamflow reconstruction indicated a pronounced reduction in streamflow in the upper Indus River basin during solar minima (Maunder, Dalton, and Damon). Shorter periods (years) of low streamflow in the reconstruction corresponded to major volcanic eruptions. Extreme low and high streamflows were also linked with sea surface temperature. The streamflow reconstruction also provides a long-term context for recent high Asian streamflow variability resulting from seasonal snow and glaciers that is critically needed for water resources management and assessment.

1. Introduction

As a result of fast-growing populations and socio-economic development, demand for water resources in South Asian countries is increasing rapidly, and water disputes are escalating in the South Asian subcontinent (Zawahri 2009, Qiu 2016, Li *et al* 2016, Zhang 2016, Reddy *et al* 2017, Vinke *et al* 2017, Biemans *et al* 2019). The uncertainty of the impact of climate change and human activities is one of the most important environmental challenges facing water supply assessment, with far-reaching implications on regional sustainable development (Wu *et al* 2017, Kundzewicz *et al* 2018). Thus, many studies have focused on the availability of water resources in various climate scenarios (Gosling and Arnell 2016,

Tramblay *et al* 2018, Yao *et al* 2019, Zhai *et al* 2020, Liu *et al* 2020). Although the South Asian monsoon generally brings abundant rainfall, the water resources of the Indian subcontinent, which is one of the most densely populated areas in the world, are unevenly distributed due to monsoon failure; as a result, South Asian countries are currently facing differing degrees of water scarcity (Cook *et al* 2010, Chen *et al* 2017, Mishra *et al* 2019, Zhai *et al* 2020). Increased meltwater from high Asian glaciers resulting from global warming has raised doubts about the capacity of freshwater supplies to meet the growing water demands of South Asia (Bolch 2017, Gao *et al* 2019, Pan *et al* 2019). South Asian socio-economic development has been greatly affected, either directly or indirectly, by the climate-driven changes in water resources. Thus, long-term river streamflow records are needed for proper water resource planning. Nevertheless, the brevity of the span of instrumental streamflow records available in South Asia has greatly hampered the development of appropriate water resource management policies and severely limited our understanding of South Asian water resources from a long-term perspective.

Moisture-sensitive tree-ring width series from high Asian river basins provide reliable high-resolution streamflow records dating back several centuries or even millennia (Yuan *et al* 2007, Gou *et al* 2010, Liu *et al* 2010, Yang *et al* 2012, Cook *et al* 2013, Singh and Yadav 2013, Shah *et al* 2014, Xiao *et al* 2017, Panyushkina *et al* 2018, Rao *et al* 2018, Chen *et al* 2019a, 2019b, Zhang *et al* 2020). Tree-ring width chronologies of conifers from the Indus River basin, which is one of the most important irrigation water sources in South Asia, have been used to develop streamflow reconstructions (Cook *et al* 2013, Rao *et al* 2018). By using a network of tree-ring sites from the upper Indus basin, including a large number of climate-sensitive tree-ring width series, precipitation- and temperature-related mixed streamflow data have been reconstructed, and thus can effectively reveal the history of the Indus River in terms of water resources (Rao *et al* 2018). Both the South Asian summer monsoon and glacial changes have significant effects on the streamflow of the Indus River (Koppes *et al* 2015, Mukhopadhyay and Khan 2015, Minallah and Ivanov 2019), but the effects of these factors on the streamflow have not been quantitatively established.

In this study, we develop a new tree-ring width chronology of the Himalayan white pine (*Pinus wallichiana*) from an upper-treeline site in Northern Pakistan, and apply the reliable period of this chronology to reconstruct June–July streamflow variations in the Indus River since 1350 CE. We use this reconstruction to investigate high Asian streamflow variability resulting from seasonal snow and glacier ice. We also explore the streamflow variations in relation to natural forcings. In particular, we focus on the relationship between streamflow changes and the historical process in South Asia.

2. Materials and methods

2.1. Study area

The sampling site (AST, 74°48′ E, 35°20′ N, 3450–3500 m a.s.l.) is located in arid and semi-arid regions in Northern Pakistan (figure 1), lies in the path of the westerly and South Asian monsoon is often affected by water vapour transport anomalies (Latif *et al* 2017, Bibi *et al* 2020). These characteristics make the region sensitive to climate change (e.g. Anjum *et al* 2019). Precipitation may exceed 1000 mm at the windward slopes near the upper treeline (Ahmed *et al* 2017); the region surrounding Astore (and the sampling site from which tree-ring cores were collected) was actually more similar to the sub-humid plateau monsoon regions based on variations in precipitation and temperature. As a result, high-altitude areas in the regions are characterised by cold, snowy winters and warm, wet summers, and covered by widespread glaciers and a wide variety of coniferous forests. Mean annual temperature and precipitation values equal approximately 486.2 mm and 9.9 °C, respectively (figure 2(A)). Average May–June precipitation and temperature range from 7.9 to 150.1 mm and from 16.7 °C to 21.8 °C, respectively. The Indus River valleys in the study area are characterised by arid and semi-arid climates (with 139 mm of precipitation in Gilgit). Seasonal distributions of streamflow and precipitation differ somewhat, and streamflow increase rapidly from June to August because of the influence of snow/glacier meltwater (figure 2(B)). High correlations among the instrumental streamflow records indicated that the streamflow of different rivers at the upper Indus River basin was responding to common factors (figure 2(C)).

2.2. Tree-ring data

One tree-ring site (AST) was sampled in the Astore region (figure 1). Increment cores were collected from living Himalayan white pine trees at breast height, using 10 mm-diameter increment borers. In total, 75 increment cores were collected from 37 trees from the AST site at the upper treeline near the glaciers in the Astore region. The biophysical environment implies that the growth of Himalayan white pine is limited by temperature at the timberline in the Karakoram (Asad *et al* 2017). All increment cores were mounted and polished with 400 grit sandpaper; annual ring widths were measured to the nearest 0.01 mm using a LINTAB measuring system. We used the COFECHA program to assess the cross-matching quality of all tree-ring width series (Holmes 1983). Next, we standardised all individual tree-ring width

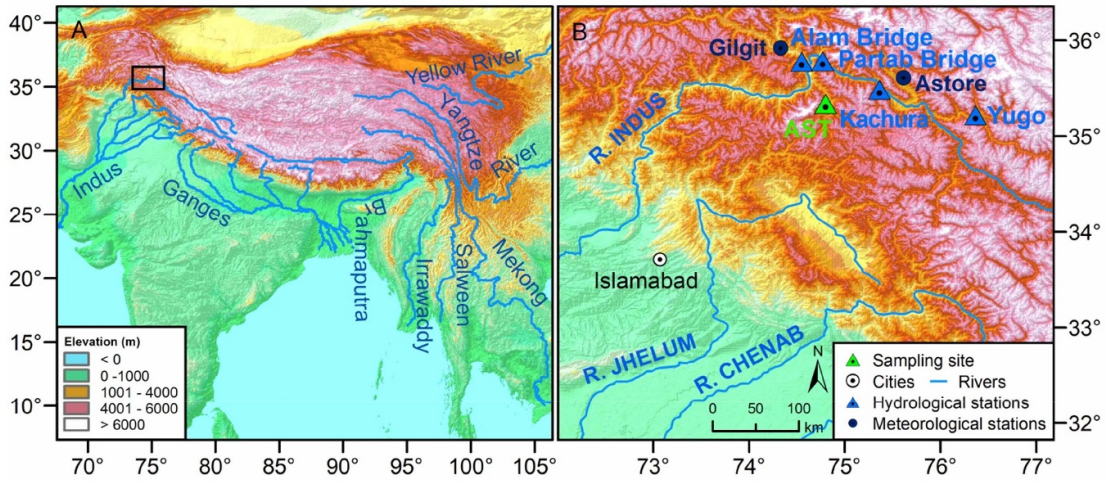

Figure 1. (A) Map showing major rivers originating on the Tibetan Plateau, the black rectangle indicates the area of detailed research in the upper Indus River, northern Pakistan. (B) Locations of the sample site, hydrological stations and climate stations in the upper Indus River.

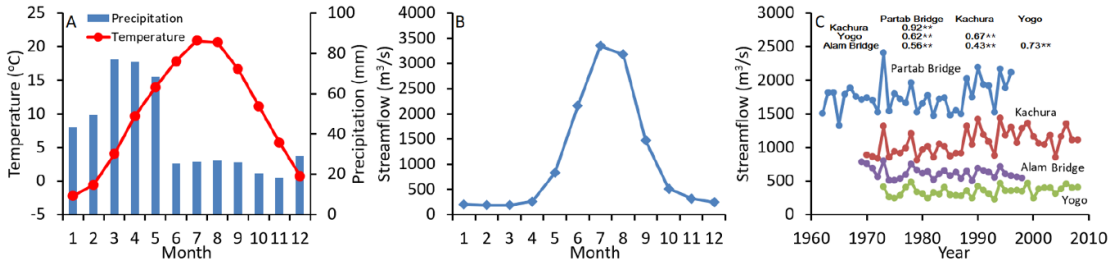

Figure 2. (A) Monthly mean temperature and monthly total precipitation at the Astore meteorological station (1972–2017 CE). (B) The average monthly streamflow from 1970 to 2008 at the Kachura hydrologic station. (C) The annual streamflow records from the Partab Bridge (Indus River, 1962–1996), Kachura (Indus River, 1970–2008), Yogo (Shyok River, 1973–2008) and Alam Bridge (Gilgit River, 1969–1998).

series, using the ARSTAN program, by conservative de-trending methods (negative exponential and straight-line curve fits) to remove non-climatic trends due to tree age and tree size while minimizing the removal of the climatic variance (Cook 1985). The detrended series were combined into the site chronology using a biweight robust mean (Cook 1985). We chose to use the standard version of the tree-ring width chronology (AST), ranging from low- to high-frequency common signals, which includes environmental and climatic signals. A minimum sample depth (number of trees $\geqslant 3$) was adopted to ensure that strong climate or hydrological signals were based on years when the expressed population signal (EPS) was higher than 0.85 (Wigley *et al* 1984). The AST chronology used in the streamflow reconstruction below was therefore truncated prior to 1350 CE, based on the threshold values.

2.3. Instrumental data and statistical methods

Monthly instrumental climate data from 1972 to 2017, included monthly mean temperature and total monthly precipitation, were obtained for the Astore climate station (74°20′ E, 35°55′ N, 1454 m a.s.l.) from the Pakistan meteorological department (figure 2(A)). Monthly mean streamflow data of the upper Indus River were obtained from the Kachura hydrological station, located at 75°25′ E, 35°27′ N, 2341 m a.s.l. (table 1). The streamflow records date from 1970 to 2008. Figure 2(B) shows the average monthly streamflow from 1970 to 2008 at the Kachura hydrologic station. Other instrumental streamflow data were also obtained from three hydrological stations, Partab Bridge (Indus River, 1962–1996), Yogo (Shyok River, 1973–2008), and Alam Bridge (Gilgit River, 1969–1998), showing the existence of some strong signals common to several hydrological stations (figure 2(C)). Bootstrapped correlation analysis was performed for initial indication of the relationship between tree growth and monthly streamflow/climate using the DENDROCLIM2002 program (Biondi and Waikul 2004), for which data were available without gaps. As seasonally averaged climate and streamflow is more representative than just one single month (Fritts 1976), we also screened the AST chronology in simple correlation analysis (Pearson's correlation) with the seasonal climate and streamflow subsets to find the most appropriate

Table 1. Site information of sampling site, streamflow gauge network climate and climate station, and statistics for the tree-ring chronology.

Site/ chro.names	Long (E)	Lat (N)	Elevation (m a.s.l.)	Slope inclination	Exposure	Core/ tree number	Length of chronology	MS	SD	AC1	SNR	VFE	EPS
AST	74°48′	35°20′	3450–3500	5°-20°	0.2	75/37	1317–2017	0.12	0.15	0.52	13.97	30.5%	0.93
Partab Bridge	74°38′	35°47′	1419				1962–1996						
Kachura	75°25′	35°27′	1969				1970–2008						
Yogo	76°06′	35°11′	2469				1973–2008						
Alam Bridge	74°36′	35°46′	1966				1969–1998						
Astore	74°20′	35°55′	1454				1972–2017						

Note: MS is the mean sensitivity; SD is the standard deviation; AC1 is the autocorrelation order 1; SNR is the signal-to-noise ratio; VFE is the variance in first eigenvector; EPS is the expressed population signal.

seasonal predictand for the streamflow reconstruction. To examine the lagged effects of prior-year climate/streamflow on subsequent ring formation, the analysis window was extended from previous July to September of the current year.

Considering the importance of understanding historical summer streamflow in Indus River and the highest correlation coefficient, standard tree-ring methods were used to reconstruct June–July streamflow for the upper Indus River basin (Fritts 1976). The linear regression model between the predictors (the AST chronology) and the predictand (streamflow) was then developed, retrodicting streamflow data during the pre-instrumental period. Because the instrumental streamflow record is not long enough to be divided into the verification and calibration periods, we used the 'leave-one-out' method (Michaelsen 1987) to assess the statistical fidelity of our reconstruction equation. The statistics include the Pearson's correlation coefficient, reduction of error, sign test and product mean test (Fritts 1976). To verify whether the reconstruction is subjected to over-fitting due to trend distortion, we also calibrated the first differences (year-to-year changes) of the tree-ring series with actual streamflow data. A temperature-sensitive streamflow reconstruction of Kara Darya River in the Pamir-Alai Mountains, Kyrgyzstan (Zhang *et al* 2020), provides a reference to validate our streamflow reconstruction.

In order to establish whether our streamflow reconstruction exhibited links with large-scale temperature and snow cover, we correlated our streamflow reconstruction with the June–July snow cover dataset (1966–2017) (https://climate.rutgers.edu/snowcover) and HadCRUT4/HadSST4 (Cowtan and Way 2014) June–July temperature (1960−2017). Finally, in order to investigate teleconnections of regional streamflow to remote oceans, the two composite sea surface temperature (SST) anomaly maps of the 10 highest and the 10 lowest streamflow years during the period 1948–2017 were created using the gridded SST dataset (Smith and Reynolds 2003) to indicate the different spatial SST pattern.

In order to indicate the periodicities of our streamflow reconstruction, we performed a multitaper method (MTM) analysis (Mann and Lees 1996) with a $5 \times 3\ \pi$ taper and a red noise background. MTM is an good method for investigating periodicities of the time sequence because it requires very few *a priori* assumptions concerning the structure of the time sequence, and provides a robust average values for separating the signal and noise components of the time sequence. To reveal possible influence of solar activity on regional streamflow, we compared with the streamflow reconstruction, using solar activity reconstruction (Muscheler *et al* 2007), sunspot numbers (www.sidc.be/silso/datafiles) and Northern Hemisphere summer temperature reconstruction (Wilson *et al* 2016, Guillet *et al* 2017).

To determine the impact of volcanic-induced cooling on the high Asian seasonal snow and glacier-derived streamflow, we also applied a superposed epoch analysis (SEA, Haurwitz and Brier 1981). A total of 48 primarily volcanic eruption events with high volcanic eruption indexes (VEI $\geqslant 5$) prior to the 1990s was downloaded from the Smithsonian Institution (http://volcano.si.edu/search_eruption.cfm). In SEA each year in a list of primarily volcanic eruption events is taken as the zero window year. Streamflow values for the volcanic event years and for windows of years, in this case 6 years before and 4 years after the volcanic event years, are expressed as departures from the average values for the 11 years in each case. The departures for all the 11 years windows are averaged and superposed. The Monte Carlo simulation technique was used to evaluate the statistical significance of autocorrelation of the streamflow reconstruction with the random sampling method (Adams *et al* 2003). SEA was conducted using the EVENT software (version 6.02P) (www.ltrr.arizona.edu/software.html).

3. Results

Comparison between the AST chronology and monthly streamflow indicate the existence of significant positive correlations during early summer (from June to July) (figure 3(A)). Further analysis showed that the tree-ring width chronology is more significantly correlated with temperature, and conversely, that there is no significant correlation with precipitation (figure 3(B)). A significant correlation ($r = 0.47$, $P < 0.01$) was found between the AST chronology and the mean temperature from the previous October to the current July; the highest correlation ($r = 0.64$, $P < 0.01$) occurred between the tree-ring width chronology and the June–July period, implying that the temperature-sensitive tree-ring width chronology could be used as an indicator of temperature-dominated ice-snow meltwater signals (Starheim *et al* 2013, Zhang *et al* 2020).

The AST chronology explains 40.9% of the instrumental June–July streamflow variance during the period 1972–2008. Thus, the AST chronology was used in the regression model to reconstruct the June–July streamflow of the upper Indus River. The final connection between this streamflow as a transfer function of tree-ring widths designed by regression analysis is shown below:

$$Y = -368.24 + 3097.965X \quad (1)$$

where Y is the June–July streamflow of the upper Indus River ($m^3\ s^{-1)}$ and X is the AST chronology (non-dimensional values).

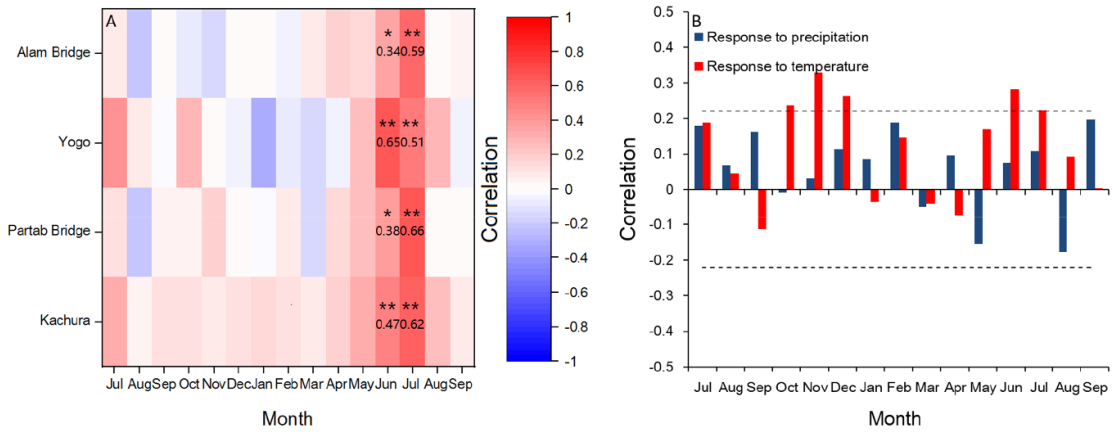

Figure 3. (A) Bootstrapped correlations of the AST chronology with monthly streamflow values of the hydrologic stations from the upper Indus River basin. * Significant at $P < 0.05$; ** significant at $P < 0.01$. (B) Bootstrapped correlations between the AST chronology and climate factors: the monthly total precipitation (blue) and monthly mean temperature (red) from the previous July to September during the common period 1972–2017. Dashed lines indicate the 0.05 significance level.

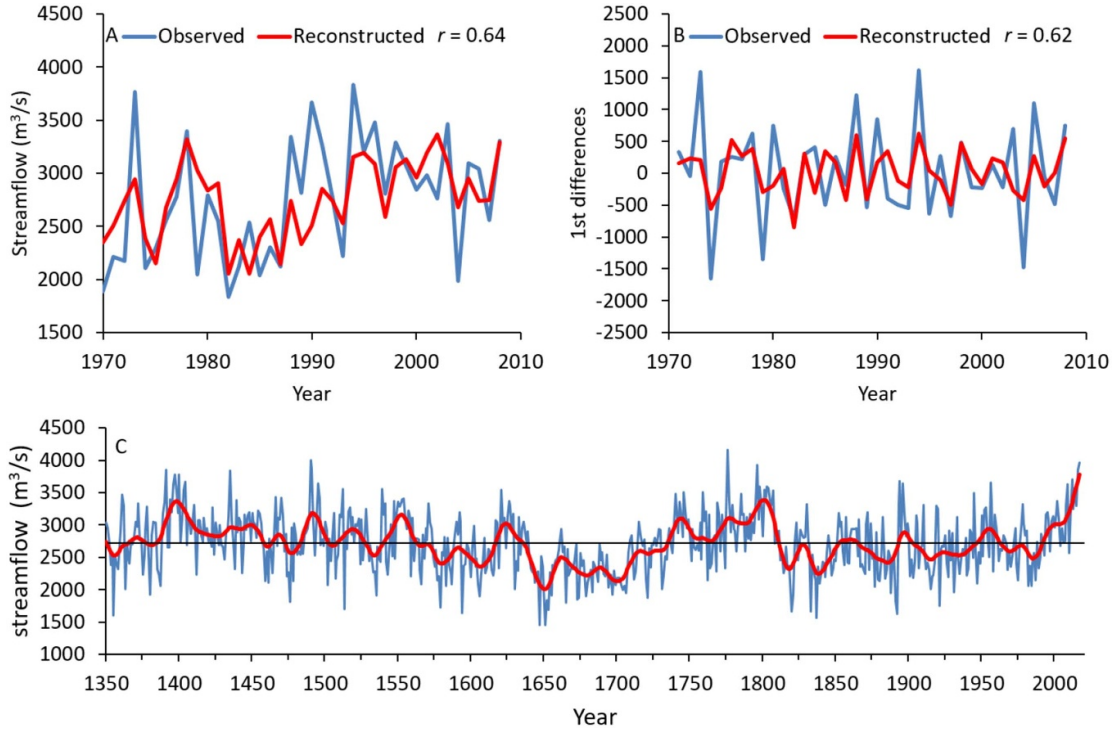

Figure 4. (A) Comparison between the observed and reconstructed June–July streamflow of the upper Indus River for the common period 1970–2008. (B) Comparison between the first differences of observed and reconstructed June–July streamflow of the upper Indus River for the common period 1970–2008. (C) June–July streamflow reconstruction of the upper Indus River since 1350 CE. The dashed horizontal line represents the long-term mean. The thick line emphasizes the long-term fluctuations of the streamflow reconstruction with a 21 year low-pass filter.

For the instrumental period (1970–2008) of the final streamflow reconstruction, the adjusted r^2 value was 0.396; the correlation between the initial differences of the tree-ring series and instrumental streamflow was 0.62 ($P < 0.01$) (figures 4(A) and (B)). The standard error of the estimate was 439.8; the F value was 25.65. The reduction of error (0.35) was strongly positive, using leave-one-out method validation, indicating the reconstructed equation was stable. For additional verification, the product means test statistics (5.49) and sign test (9–/30^+) were both found to be significant at a 99% confidence level. These tests indicated the validity of the regression model and can be used to show the June–July streamflow variations of the upper Indus River during the period 1350–2017 CE.

The June–July streamflow reconstruction and its 21 year low-pass filtered values for the upper Indus River in the northern Pakistan are shown in figure 4(C). The streamflow reconstruction included

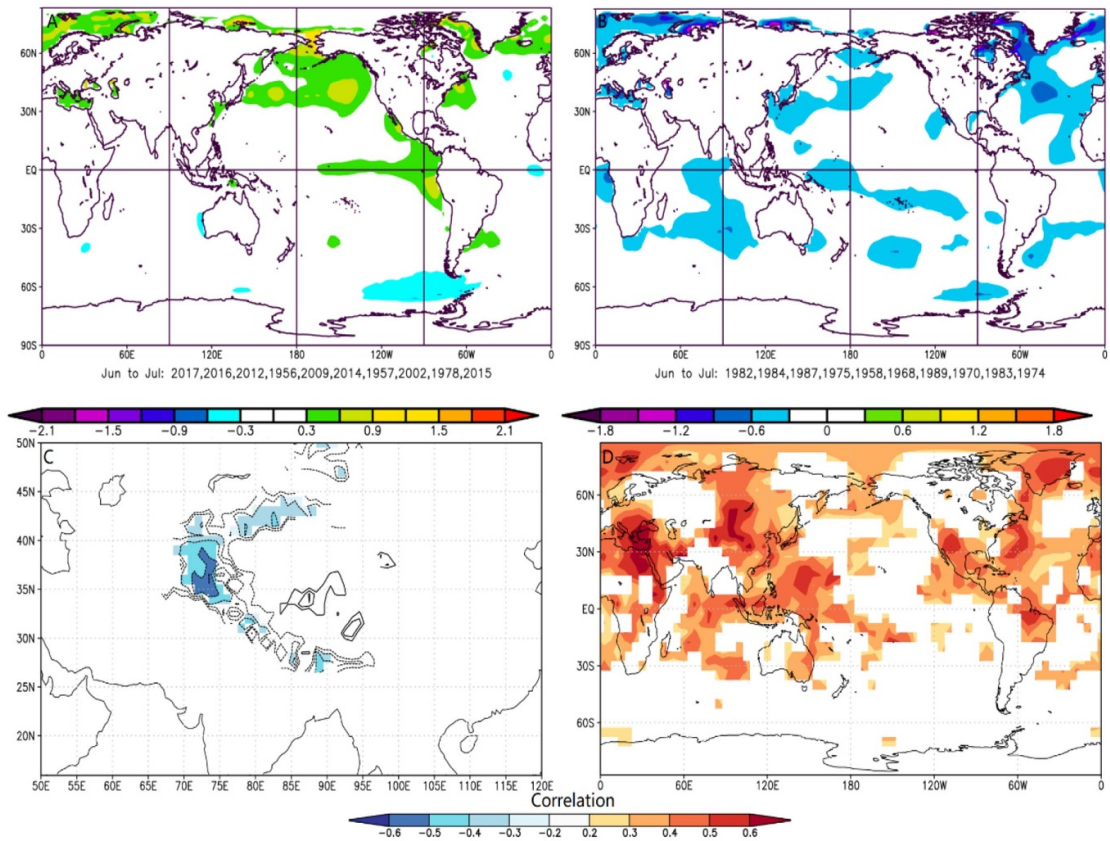

Figure 5. Composite maps of SST for the 10 highest streamflow (A) and 10 lowest streamflow (B) years. (C) Spatial correlation map of the streamflow reconstruction with the June–July snow cover dataset (https://climate.rutgers.edu/snowcover) from 1966 to 2017. (D) Spatial correlation map of the streamflow reconstruction with HadCRUT4/HadSST4 (Cowtan and Way 2014) June–July temperatures from 1960 to 2017.

a considerable number of low-frequency signals over the past 668 years. The long-term average of the streamflow reconstruction was 2716.0 m^3 s^{-1}, with a standard deviation of 454.4 m^3 s^{-1}. The streamflow reconstruction indicated relatively high streamflow from the mid-fourteenth to mid-sixteenth centuries, followed by two centuries, centred around 1650, of relatively low streamflow and pronounced high streamflow from 1750 to 1800. Streamflow over the past 200 years has generally shown a slow upward trend, with some short-term fluctuation in periods such as the 1810s through the 1850s, the 1870 through the 1890s, and the 1960s through the 1980s. The reconstructed streamflow showed an accelerating upward trend during the recent warming period.

The list of the highest and lowest streamflows reconstructed for the upper Indus River watershed since 1350 CE showed that seven of the ten lowest streamflows occurred during the seventeenth and nineteenth centuries, with the two lowest values in 1647 and 1651. Three of the ten highest streamflows occurred during the last 10 years, particularly in 2016–17. The composite map of the 10 highest streamflow years were characterised by a pattern of Tropical Eastern Pacific and mid-high latitudes SST above the average (1981–2010, 2000), resembling the pattern of El Niño years. During the 10 lowest streamflow years, the opposite pattern occurred (figures 5(A) and (B)). As shown in figure 5(C), some significant negative areas of correlation with the Rutgers snow cover dataset (https://climate.rutgers.edu/snowcover) were found in the Karakoram region. Conversely, the streamflow reconstruction was significantly positively correlated with June–July temperatures in high Asia (figure 5(D)).

The MTM of spectral analysis revealed 334 year (99%), 51.2 year (99%), 5.1 year (95%), 3.3 year (99%), and 2.2 year (99%) cycles in the reconstructed streamflow data for the upper Indus River basin. Correlations between this study and August–September Kara Darya River streamflow reconstruction (Zhang *et al* 2020), computed over the 1411–2016 common period, equalled 0.21 ($P < 0.01$), increasing to 0.32 following 40 year smoothing. Analysis of correlations between our streamflow reconstruction and solar activity revealed no systematic connection; this is likely related to the complex forcing data and regional hydroclimatic variation. Detailed comparison, however, revealed some primarily low streamflow periods (relatively low temperatures) following prominent solar minima (Maunder, Dalton and Damon) with an observed sunspot number sequence (Stuiver and

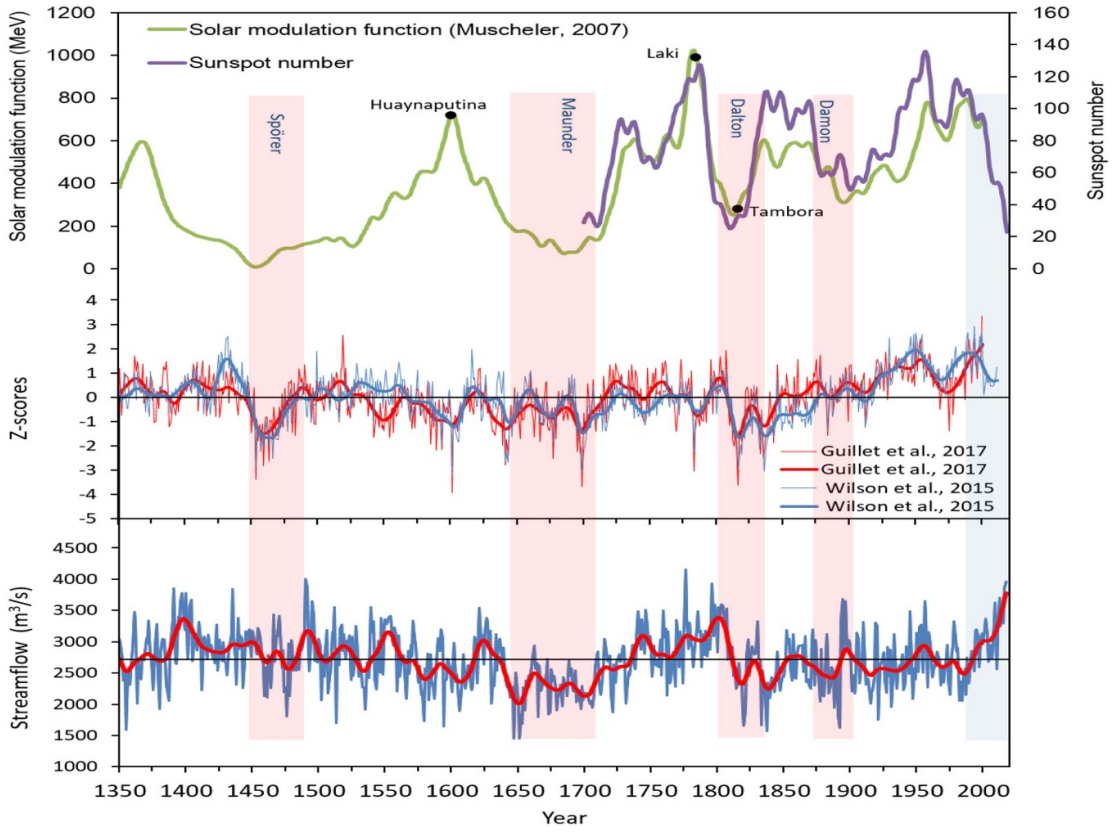

Figure 6. Comparison among streamflow reconstruction of the upper Indus River (this study), solar activity (Muscheler *et al* 2007), sunspot numbers (www.sidc.be/silso/datafiles) and Northern Hemisphere summer temperature reconstruction (Wilson *et al* 2016, Guillet *et al* 2017). All series were smoothed with a 21 year low-pass filter to emphasize long-term fluctuations. Red boxes represent low streamflow conditions during during solar minimum periods, and blue box represent out-of-phase relationship between streamflow and sunspot number during the recent warm period.

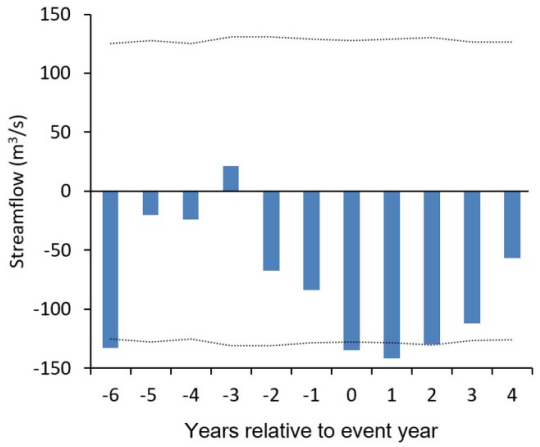

Figure 7. Results of the SEA using the significance tests (random sampling).

Braziunas 1989; figure 6). Mean streamflow during the three solar minimum periods was 6.4% lower than the long-term average of the streamflow reconstruction during the period 1350–2017. Figure 7 shows the SEA results based on a list of 48 volcano years. A statistically significant ($P < 0.01$) reduction in June–July streamflow began in the same year as the eruption and lasted for 2–4 more years. We estimated mean peak streamflow decline due to these large volcanic eruptions at 134–141 $m^3\ s^{-1}$.

4. Discussion

4.1. Tree growth/streamflow relationships

Most previous dendroclimatic reconstructions of river streamflows have been based on precipitation/moisture-sensitive tree-ring-width series (Yuan *et al* 2007, Akkemik *et al* 2008, Gou *et al* 2010, Liu *et al* 2010, Urrutia *et al* 2011, Yang *et al* 2012, Singh and Yadav 2013, Shah *et al* 2014, Woodhouse and Pederson 2018, Chen *et al* 2019a, 2019b). Due to multiple streamflow contributions caused by the complex mountain terrain of Karakorum, the development of streamflow reconstructions for the upper Indus River basin requires a dense multi-species tree-ring network which is related to both precipitation and temperature, and the highest positive correlation between tree-ring widths and monthly streamflow were found in the current growing season (May–September) (Cook *et al* 2013, Rao *et al* 2018). The dissimilar responses of tree rings to streamflow indicate that multi-species tree-ring networks from different environments can be used to capture multiple-season streamflow signals (Cook *et al*

2013), whereas site chronology captures mostly the link between hydrological information and a single climatic element (the present study). Due to the scarcity of summer precipitation, the streamflow in this period originates mainly from winter precipitation and glaciers (figure 2(A)). These streamflow reconstructions provided us with accurate hydrological information for the upper Indus River basin (Cook *et al* 2013, Rao *et al* 2018); however, this information cannot, due to the positive linkages between precipitation and tree-ring-width series, reflect temperature-dominated ice-snow meltwater signals (Rao *et al* 2018). Hydrologic information concerning temperature-related ice-snow meltwater is of great significance for revealing the mechanism governing high Asian Alpine glacier water resources in the context of global warming (Smith and Bookhagen 2018, Armstrong *et al* 2019, Farinotti *et al* 2020), especially for the Indian subcontinent, with its severe water shortage.

In the past decade, some warm-season streamflow reconstructions have been developed using temperature-sensitive tree-ring sequences (Hart *et al* 2010, Starheim *et al* 2013, Zhang *et al* 2020). We extended previously indicated complex linkages between tree-ring widths and climate/streamflow; additionally, although the AST chronology has no significant correlation with precipitation, we confirmed its relationship with ice-snow meltwater based on high sensitivity to temperature, including SST (figures 5(A) and (B)). From these relationships, we developed our reconstruction model of the upper Indus River June–July streamflow. Our models demonstrate that temperature-sensitive tree-ring sequences can be used to reconstruct warm-season streamflow in high Asia. Although responses of tree rings to streamflow and climate are inconsistent, a close correlation ($r = 0.47$, $P < 0.01$) between this study and that of Rao *et al* (2018) was found for the period 1394–2005 CE. The significant negative correlation with the Rutgers snow cover dataset (Kunkel *et al* 2016) also indicates that the streamflow reconstruction may reflect temperature-dominated ice-snow meltwater, and an increase in June–July streamflow was often accompanied by a reduction in snow cover. However, due to the complex geographical environment of high Asia and the influence of the Asian summer monsoon, linkage between temperature-sensitive tree-ring series and streamflow appears to exist in the western part of high Asia, where summer rainfall is scarce.

4.2. Natural forcings

Solar activity and its associated energy transfer not only affect the earth's biology and climate, but also exert an important impact on water cycles (Friis-Christensen and Lassen 1991, Messerotti and Chela-Flores 2009, Al-Tameemi and Chukin 2016, Le Mouël *et al* 2019). As shown in figure 6, close synchronism exists between periods of significantly low streamflow and solar minima (Maunder, Dalton, and Damon). Our streamflow reconstruction exhibits a downward trend from the late Mediaeval Warm Period to the Little Ice Age (Lamb 1965). In particular, streamflow decreased by about 16.1% under the cold conditions during the Maunder Minimum (1645–1715), implying that the output of high Asian Alpine glaciers in terms of water output was governed by solar activity during past centuries, notwithstanding the dramatic changes in this relationship in the recent warm period. In addition to providing tree-ring evidence for decreases in meltwater due to low temperature during the three solar minima, we also found that the solar maximum was synchronised with the high streamflow stage, with a lag of 20–40 years. This lag effect may be linked with unexplained variance in tree rings and other forcing factors, such as volcanic eruptions. The out-of-phase relationship since the 1980s likely refers to anthropogenic warming (Cook *et al* 2016, Santer *et al* 2019), although the issue of human contributions to recent warming is an open question (Hoegh-Guldberg *et al* 2019, Connolly *et al* 2020). The interaction between solar activity and anthropogenic warming complicates high Asian streamflow variability.

Many studies have revealed that large volcanic eruptions have had important effects on summer temperatures (Anchukaitis *et al* 2012, D'Arrigo *et al* 2013, Duan *et al* 2018, Liang *et al* 2019); meanwhile, volcanic-induced cooling may cause changes in glacier mass balance and water cycles (Rampino and Self 1992, Iles and Hegerl 2015, Van Der Bilt *et al* 2019, Huston *et al* 2021). Our streamflow reconstruction revealed that large volcanic eruption events may have resulted in reduced streamflow in the upper Indus River basin (figure 7). A previous study had shown that volcanic eruptions caused a reduction in pre-monsoon precipitation in high Asia (Liang *et al* 2019); our study further confirmed that volcanic-induced cooling also led to a corresponding reduction in meltwater in subsequent months. The combination of the two effects may lead to a reduction in the annual streamflow output of high Asia. For the upper Indus River basin, the most pronounced volcanic radiative forcing arose from a series of large volcanic eruptions between the 1800s and 1810s (Sigurdsson and Carey 1989, Oppenheimer 2003), including the 1815 eruption of Tambora (Chenoweth 2001, Raible *et al* 2016). This low streamflow period likely resulted in a volcanic-induced cooling effect, along with lower temperatures due to a low level of solar activity in the Dalton Minimum (Russell *et al* 2010). Large volcanic eruptions also correspond to the delayed emergence of high streamflow during the sunspot maximum, including Huaynaputina (1600, VEI = 6; De Silva and Zielinski 1998), Laki (1783, VEI = 5; Thordarson and Self 2003), and Tambora (1815, VEI = 7; Raible *et al* 2016). Overall, low-frequency signals

of streamflow reconstruction appear to mimic solar activity; moreover, the timing of large volcanic eruptions matches certain low streamflow events, possibly exacerbating Indian subcontinent water scarcity. Interestingly, large volcanic eruptions may delay the appearance of high streamflow during solar maxima, and the irregular nature of large-scale volcanic eruptions may have led to some errors in the streamflow project. Recent anthropogenic warming has not only further diminished the influence of natural forcing during the modern warm period (Park *et al* 2018, Marvel *et al* 2019), but also changed the high Asian water cycle.

4.3. Interaction between streamflow and human activities

Although summer streamflow in this region and in Central Asia are in close agreement, drought and low streamflow events occurred in Central Asia from the late fifteenth to the early sixteenth century (Opała-Owczarek and Niedźwiedź 2019, Zhang *et al* 2020). This dry condition forced Central Asian peoples to migrate outwards, while the neighbouring Indian subcontinent, including the Indus basin, was relatively humid and attracted conquerors from Central Asia (Yadava *et al* 2016). It is interesting to note the low streamflow phase during the Maunder Minimum (1645–1715). Famine and the economic hardships caused by bad climate during the Maunder Minimum forced the Mughal emperors to undertake the conquests to relieve the Empire's ruling crisis (Panhwar 2004, Uberoi 2012, Parwez and Khan 2017) The Mughal Empire, although it reached its maximum extent under Aurangzeb, was slowly weakened by prolonged low streamflow and frequent warfare (Truschke 2017). Despite high streamflows during the eighteenth century due to relatively high temperatures (Yadav *et al* 2011), the Indian subcontinent was conquered completely only after the early-nineteenth-century low streamflow (Clingingsmith and Williamson 2008). We must admit that streamflow is not the decisive factor in the historical process; nevertheless, it has affected regional social and economic development to a certain extent. Based on our tree-ring record, streamflow, unusually, has increased by 18.3% over the past 20 years. Streamflow in the Indian subcontinent may have benefitted from recent anthropogenic warming (Lutz *et al* 2014, Armstrong *et al* 2019); however, this increase was based on the rapid melting of glaciers, and this area is marked by great uncertainty (Luo *et al* 2018, Biemans *et al* 2019). Correlations between this study and temperature under the CMIP6 SSP-585 scenario (CESM2, Eyring *et al* 2019), computed over the 1850–2017 common period are 0.36, and increase to 0.59 after 21 year smoothing. Since the streamflow is mainly controlled by temperature, according to the linear model, the averaged streamflow will risen by more than 35% during the period 2018–2100. However, if anthropogenic warming continues and glaciers disappear, a significant reduction in streamflow (Kraaijenbrink *et al* 2017, Pritchard 2019) may occur; this may have a negative impact on the Indian subcontinent (Biemans *et al* 2019), which is densely populated and depends heavily on snow and ice melt for irrigation agriculture.

5. Conclusions

In this paper, a new tree-ring chronology of *Pinus wallichiana* was developed from the upper Indus River basin in Northern Pakistan. The tree-ring chronology is sensitive to October–July temperature variations, and has a strong association with streamflow changes. Based on this temperature-sensitive chronology, we have presented a well-calibrated and verified June–July streamflow reconstruction of the upper Indus River basin. This streamflow reconstruction placed the unusual and unprecedented most recent upward trend of snow- and glacier-melt-driven streamflow since the 1990s in a long-term context and enabled evaluation of potential impacts of water resources on historical societal changes on the Indian subcontinent. This streamflow reconstruction also enabled an assessment of the possible effect of solar activity and large volcanic eruptions on the variability of high Asian streamflow from seasonal snow and glacier ice.

Data availability statement

The data that support the findings of this study are available upon reasonable request from the authors.

Acknowledgments

This work was supported by the 2nd Scientific Expedition to the Qinghai-Tibet Plateau (No. 2019QZKK010206), NSFC (U1803341) and the National Key R&D Program of China (2018YFA0606401).

ORCID iDs

Magdalena Opała-Owczarek https://orcid.org/0000-0002-0583-6443
Piotr Owczarek https://orcid.org/0000-0001-7877-7731

References

Adams J B, Mann M E and Ammann C M 2003 Proxy evidence for an El Nino-like response to volcanic forcing *Nature* **426** 274–8

Ahmed K, Shahid S, Chung E S, Ismail T and Wang X J 2017 Spatial distribution of secular trends in annual and seasonal precipitation over Pakistan *Clim. Res.* **74** 95–107

Akkemik Ü, D'Arrigo R, Cherubini P, Köse N and Jacoby G C 2008 Tree-ring reconstructions of precipitation and streamflow for north-western Turkey *Int. J. Climatol.* **28** 173–83

Al-Tameemi M A and Chukin V V 2016 Global water cycle and solar activity variations *J. Atmos. Sol. Terr. Phys.* **142** 55–59
Anchukaitis K J, Breitenmoser P, Briffa K R, Buchwal A, Büntgen U, Cook E R and Grudd H 2012 Tree rings and volcanic cooling *Nat. Geosci.* **5** 836–7
Anjum M N, Ding Y and Shangguan D 2019 Simulation of the projected climate change impacts on the river flow regimes under CMIP5 RCP scenarios in the westerlies dominated belt, northern Pakistan *Atmos. Res.* **227** 233–48
Armstrong R L, Rittger K, Brodzik M J, Racoviteanu A, Barrett A P, Khalsa S J S and Kayastha R B 2019 Runoff from glacier ice and seasonal snow in high Asia: separating melt water sources in river flow *Reg. Environ. Change* **19** 1249–61
Asad F, Zhu H, Zhang H, Liang E, Muhammad S, Farhan S B, Hussain L, Wazir M, Ahmed M and Esper J 2017 Are Karakoram temperatures out of phase compared to hemispheric trends? *Clim. Dyn.* **48** 3381–90
Bibi A, Ullah K, Yushu Z, Wang Z and Gao S 2020 Role of westerly jet in torrential rainfall during monsoon over Northern Pakistan *Earth Space Sci.* **7** e2019EA001022
Biemans H, Siderius C, Lutz A F, Nepal S, Ahmad B, Hassan T and Immerzeel W W 2019 Importance of snow and glacier meltwater for agriculture on the Indo-Gangetic Plain *Nat. Sustain.* **2** 594–601
Biondi F and Waikul K 2004 DENDROCLIM2002: a C++ program for statistical calibration of climate signals in tree-ring chronologies *Comput. Geosci.* **30** 303–11
Bolch T 2017 Hydrology: Asian glaciers are a reliable water source *Nature* **545** 161–2
Carey S and Sigurdsson H 1989 The intensity of plinian eruptions *Bull Volcanol* **51** 28–40
Chen F, Shang H, Panyushkina I P, Meko D M, Yu S, Yuan Y and Chen F 2019a Tree-ring reconstruction of Lhasa River streamflow reveals 472 years of hydrologic change on southern Tibetan Plateau *J. Hydrol.* **572** 169–78
Chen F, Shang H, Panyushkina I, Meko D, Li J, Yuan Y and Luo X 2019b 500-year tree-ring reconstruction of Salween River streamflow related to the history of water supply in Southeast Asia *Clim. Dyn.* **53** 6595–607
Chen X, Long D, Hong Y, Zeng C and Yan D 2017 Improved modeling of snow and glacier melting by a progressive two-stage calibration strategy with GRACE and multisource data: How snow and glacier meltwater contributes to the runoff of the Upper Brahmaputra River basin? *Water Resour. Res.* **53** 2431–66
Chenoweth M 2001 Two major volcanic cooling episodes derived from global marine air temperature, AD 1807–1827 *Geophys. Res. Lett.* **28** 2963–6
Clingingsmith D and Williamson J G 2008 Deindustrialization in 18th and 19th century India: Mughal decline, climate shocks and British industrial ascent *Explor. Econ. Hist.* **45** 209–34
Connolly R, Connolly M, Carter R M and Soon W 2020 How much human-caused global warming should we expect with business-as-usual (BAU) climate policies? a semi-empirical assessment *Energies* **13** 1365
Cook E R 1985 A time series analysis approach to tree-ring standardization PhD Thesis University of Arizona, Tucson
Cook E R, Anchukaitis K J, Buckley B M, D'Arrigo R D, Jacoby G C and Wright W E 2010 Asian monsoon failure and megadrought during the last millennium *Science* **328** 486–9
Cook E R, Palmer J G, Ahmed M, Woodhouse C A, Fenwick P, Zafar M U and Khan N 2013 Five centuries of upper Indus River flow from tree rings *J. Hydrol.* **486** 365–75
Cook J, Oreskes N, Doran P T, Anderegg W R, Verheggen B, Maibach E W and Nuccitelli D 2016 Consensus on consensus: a synthesis of consensus estimates on human-caused global warming *Environ. Res. Lett.* **11** 048002
Cowtan K and Way R G 2014 Coverage bias in the HadCRUT4 temperature series and its impact on recent temperature trends *Q. J. R. Meteorol. Soc.* **140** 1935–44
D'Arrigo R, Wilson R and Anchukaitis K J 2013 Volcanic cooling signal in tree ring temperature records for the past millennium *J. Geophys. Res.* **118** 9000–10
De Silva S L and Zielinski G A 1998 Global influence of the AD 1600 eruption of Huaynaputina, Peru *Nature* **393** 455–8
Duan J, Li L, Ma Z, Esper J, Büntgen U, Xoplaki E and Luterbacher J 2018 Summer cooling driven by large volcanic eruptions over the Tibetan Plateau *J. Clim.* **31** 9869–79
Eyring V *et al* 2019 Taking climate model evaluation to the next level *Nat. Clim. Change* **9** 102–10
Farinotti D, Immerzeel W W, De Kok R J, Quincey D J and Dehecq A 2020 Manifestations and mechanisms of the Karakoram glacier anomaly *Nat. Geosci.* **13** 8–16
Friis-Christensen E and Lassen K 1991 Length of the solar cycle: an indicator of solar activity closely associated with climate *Science* **254** 698–700
Fritts H 1976 *Tree-rings and Climate* (New York: Academic) pp 567
Gao J, Yao T, Masson-Delmotte V, Steen-Larsen H C and Wang W 2019 Collapsing glaciers threaten Asia's water supplies (https://doi.org/10.1038/d41586-018-07838-4)
Gosling S N and Arnell N W 2016 A global assessment of the impact of climate change on water scarcity *Clim. Change* **134** 371–85
Gou X, Deng Y, Chen F, Yang M, Fang K, Gao L and Zhang F 2010 Tree ring based streamflow reconstruction for the upper Yellow River over the past 1234 years *Chin. Sci. Bull.* **55** 4179–86
Guillet S, Corona C, Stoffel M, Khodri M, Lavigne F, Ortega P and Oppenheimer C 2017 Climate response to the Samalas volcanic eruption in 1257 revealed by proxy records *Nat. Geosci.* **10** 123–8
Han P, Long D, Han Z, Du M, Dai L and Hao X 2019 Improved understanding of snowmelt runoff from the headwaters of China's Yangtze River using remotely sensed snow products and hydrological modeling *Remote Sensing of Environment* **224** 44–59
Hart S J, Smith D J and Clague J J 2010 A multi-species dendroclimatic reconstruction of Chilko River streamflow, British Columbia, Canada *Hydrol. Process.* **24** 2752–61
Haurwitz M W and Brier G W 1981 A critique of the superposed epoch analysis methoddits application to solar–weather relations *Mon. Wea. Rev.* **109** 2074–9
Hoegh-Guldberg O, Jacob D, Taylor M, Bolaños T G, Bindi M, Brown S and Engelbrecht F 2019 The human imperative of stabilizing global climate change at 1.5 C *Science* **365** eaaw6974
Holmes R L 1983 A computer-assisted quality control program *Tree-Ring Bull.* **43** 69–78
Huston A, Siler N, Roe G H, Pettit E and Steiger N J 2021 Understanding drivers of glacier length variability over the last millennium *Cryosphere Discuss.* **15** 1645–62
Iles C E and Hegerl G C 2015 Systematic change in global patterns of streamflow following volcanic eruptions *Nat. Geosci.* **8** 838–42
Koppes M, Rupper S, Asay M and Winter-Billington A 2015 Sensitivity of glacier runoff projections to baseline climate data in the Indus River basin *Front. Earth Sci.* **3** 59
Kraaijenbrink P D A, Bierkens M F P, Lutz A F and Immerzeel W W 2017 Impact of a global temperature rise of 1.5 degrees Celsius on Asia's glaciers *Nature* **549** 257–60
Kundzewicz Z W, Krysanova V, Benestad R E, Hov Ø, Piniewski M and Otto I M 2018 Uncertainty in climate change impacts on water resources *Environ. Sci. Policy* **79** 1–8
Kunkel K E, Robinson D A, Champion S, Yin X, Estilow T and Frankson R M 2016 Trends and extremes in Northern Hemisphere snow characteristics *Curr. Clim. Change Rep.* **2** 65–73
Lamb H H 1965 The early medieval warm epoch and its sequel *Palaeogeogr. Palaeoclimatol. Palaeoecol.* **1** 13–37
Latif M, Syed F S and Hannachi A 2017 Rainfall trends in the South Asian summer monsoon and its related large-scale dynamics with focus over Pakistan *Clim. Dyn.* **48** 3565–81
Le Mouël J L, Lopes F and Courtillot V 2019 A solar signature in many climate indices *J. Geophys. Res.* **124** 2600–19

Li H, Xu C Y, Beldring S, Tallaksen L M and Jain S K 2016 Water resources under climate change in Himalayan basins *Water Resour. Manage.* **30** 843–59
Liang E, Dawadi B, Pederson N, Piao S, Zhu H, Sigdel S R and Chen D 2019 Strong link between large tropical volcanic eruptions and severe droughts prior to monsoon in the central Himalayas revealed by tree-ring records *Sci. Bull.* **64** 1018–23
Liu X, Liu J, Chen S, Chen J, Zhang X, Yan J and Chen F 2020 New insights on Chinese cave δ18O records and their paleoclimatic significance *Earth-Science Reviews* **207** 103216
Liu Y, Sun J, Song H, Cai Q, Bao G and Li X 2010 Tree-ring hydrologic reconstructions for the Heihe River watershed, western China since AD 1430 *Water Res.* **44** 2781–92
Luo Y, Wang X, Piao S, Sun L, Ciais P, Zhang Y and He C 2018 Contrasting streamflow regimes induced by melting glaciers across the Tien Shan–Pamir–North Karakoram *Sci. Rep.* **8** 16470
Lutz A F, Immerzeel W W, Shrestha A B and Bierkens M F P 2014 Consistent increase in high Asia's runoff due to increasing glacier melt and precipitation *Nat. Clim. Change* **4** 587–92
Mann M E and Lees J 1996 Robust estimation of background noise and signal detection in climatic time series *Clim. Change* **33** 409–45
Marvel K, Cook B I, Bonfils C J, Durack P J, Smerdon J E and Williams A P 2019 Twentieth-century hydroclimate changes consistent with human influence *Nature* **569** 59–65
Messerotti M and Chela-Flores J 2009 Solar activity and life: a review *Acta Geophys.* **57** 64–74
Michaelsen J 1987 Cross-validation in statistical climate forecast models *J. Clim. Appl. Meteorol.* **26** 1589–600
Minallah S and Ivanov V Y 2019 Interannual variability and seasonality of precipitation in the Indus River basin *J. Hydrometeorol.* **20** 379–95
Mishra V, Tiwari A D, Aadhar S, Shah R, Xiao M, Pai D S and Lettenmaier D 2019 Drought and famine in India, 1870–2016 *Geophys. Res. Lett.* **46** 2075–83
Mukhopadhyay B and Khan A 2015 A reevaluation of the snowmelt and glacial melt in river flows within upper Indus basin and its significance in a changing climate *J. Hydrol.* **527** 119–32
Muscheler R, Joos F, Beer J, Müller S A, Vonmoos M and Snowball I 2007 Solar activity during the last 1000 yr inferred from radionuclide records *Quat. Sci. Rev.* **26** 82–97
Opała-Owczarek M and Niedźwiedź T 2019 Last 1100 yr of precipitation variability in western central Asia as revealed by tree-ring data from the Pamir-Alay *Quat. Res.* **91** 45
Oppenheimer C 2003 Ice core and palaeoclimatic evidence for the timing and nature of the great mid-13th century volcanic eruption *Int. J. Climatol.* **23** 417–26
Panhwar M H 2004 Little ice age severity in South Asia, 1600–1700 AD: break up of Mughal empire and role of Marathas in South India, Sikhs in Punjab and Kalhoras in Sindh in gaining independence and unifying their states (available at: www.panhwar.com/Adobe/article152.pdf (accessed 1 August 2021))
Panyushkina I P, Meko D M, Macklin M G, Toonen W H J, Mukhamadiev N S, Konovalov V G and Sagitov A O 2018 Runoff variations in Lake Balkhash basin, Central Asia, 1779–2015, inferred from tree rings *Clim. Dyn.* **51** 3161–77
Park B J, Kim Y H, Min S K and Lim E P 2018 Anthropogenic and natural contributions to the lengthening of the summer season in the Northern Hemisphere *J. Clim.* **31** 6803–19
Parwez M and Khan E 2017 Famines in Mughal India *Vidyasagar Univ. J. Hist.* **5** 21–45
Pritchard H D 2019 Asia's shrinking glaciers protect large populations from drought stress *Nature* **569** 649–54
Qiu J 2016 Stressed Indus River threatens Pakistan's water supplies *Nature* **534** 600–1
Raible C C, Brönnimann S, Auchmann R, Brohan P, Frölicher T L, Graf H F and Robock A 2016 Tambora 1815 as a test case for high impact volcanic eruptions: earth system effects *Wiley Interdiscip. Rev. Clim. Change* **7** 569–89
Rampino M R and Self S 1992 Volcanic winter and accelerated glaciation following the Toba super-eruption *Nature* **359** 50–52
Rao M P, Cook E R, Cook B I, Palmer J G, Uriarte M, Devineni N and Zafar M U 2018 Six centuries of upper Indus basin streamflow variability and its climatic drivers *Water Resour. Res.* **54** 5687–701
Reddy V R, Saharawat Y S and George B 2017 Watershed management in South Asia: a synoptic review *J. Hydrol.* **551** 4–13
Russell C T, Luhmann J G and Jian L K 2010 How unprecedented a solar minimum? *Rev. Geophys.* **48** RG2004
Santer B D, Fyfe J C, Solomon S, Painter J F, Bonfils C, Pallotta G and Zelinka M D 2019 Quantifying stochastic uncertainty in detection time of human-caused climate signals *Proc. Natl Acad. Sci.* **116** 19821–7
Shah S K, Bhattacharyya A and Chaudhary V 2014 Streamflow reconstruction of Eastern Himalaya River, Lachen 'Chhu', North Sikkim, based on tree-ring data of *Larix griffithiana* from Zemu Glacier basin *Dendrochronologia* **32** 97–106
Singh J and Yadav R R 2013 Tree-ring-based seven century long flow records of Satluj River, western Himalaya, India *Quat. Int.* **304** 156–62
Smith T M and Reynolds R W 2003 Extended reconstruction of global sea surface temperatures based on COADS data (1854–1997) *J. Clim.* **16** 1495–510
Smith T and Bookhagen B 2018 Changes in seasonal snow water equivalent distribution in high mountain Asia (1987–2009) *Sci. Adv.* **4** e1701550
Starheim C C, Smith D J and Prowse T D 2013 Dendrohydroclimate reconstructions of July–August runoff for two nival-regime rivers in west central British Columbia *Hydrol Process.* **27** 405–20
Stuiver M and Braziunas T F 1989 Atmospheric 14 C and century-scale solar oscillations *Nature* **338** 405–8
Thordarson T and Self S 2003 Atmospheric and environmental effects of the 1783–1784 Laki eruption: a review and reassessment *J. Geophys. Res.* **108** AAC–7
Tramblay Y, Jarlan L, Hanich L and Somot S 2018 Future scenarios of surface water resources availability in North African dams *Water Resour. Manage.* **32** 1291–306
Truschke A 2017 *Aurangzeb: The Life and Legacy of India's Most Controversial King* (Stanford: Stanford University Press)
Uberoi C 2012 Little ice age in mughal india: solar minima linked to droughts? *Eos* **93** 437–8
Urrutia R B, Lara A, Villalba R, Christie D A, Le Quesne C and Cuq A 2011 Multicentury tree ring reconstruction of annual streamflow for the Maule River watershed in south central Chile *Water Resour. Res.* **47** W06527
Van Der Bilt W G, Born A and Haaga K A 2019 Was Common Era glacier expansion in the Arctic Atlantic region triggered by unforced atmospheric cooling? *Quat. Sci. Rev.* **222** 105860
Vinke K, Martin M A, Adams S, Baarsch F, Bondeau A, Coumou D and Robinson A 2017 Climatic risks and impacts in South Asia: extremes of water scarcity and excess *Reg. Environ. Change* **17** 1569–83
Wigley T M L, Briffa K R and Jones P D 1984 On the average value of correlated time series, with applications in dendroclimatology and hydrometeorology *J. Appl. Meteorol. Clim.* **23** 201–13
Wilson R, Anchukaitis K, Briffa K R, Büntgen U, Cook E, D'arrigo R and Hegerl G 2016 Last millennium northern hemisphere summer temperatures from tree rings: part I: the long term context *Quat. Sci. Rev.* **134** 1–18

Woodhouse C A and Pederson G T 2018 Investigating runoff efficiency in upper Colorado River streamflow over past centuries *Water Resour. Res.* **54** 286–300

Wu J, Miao C, Zhang X, Yang T and Duan Q 2017 Detecting the quantitative hydrological response to changes in climate and human activities *Sci. Total Environ.* **586** 328–37

Xiao D, Shao X, Qin N and Huang X 2017 Tree-ring-based reconstruction of streamflow for the Zaqu River in the Lancang River source region, China, over the past 419 years *Int. J. Biometeorol.* **61** 1173–89

Yadav R R, Braeuning A and Singh J 2011 Tree ring inferred summer temperature variations over the last millennium in western Himalaya, India *Clim. Dyn.* **36** 1545–54

Yadava A K, Braeuning A, Singh J and Yadav R R 2016 Boreal spring precipitation variability in the cold arid western Himalaya during the last millennium, regional linkages, and socio-economic implications *Quat. Sci. Rev.* **144** 28–43

Yang B, Qin C, Shi F and Sonechkin D M 2012 Tree ring-based annual streamflow reconstruction for the Heihe River in arid northwestern China from AD 575 and its implications for water resource management *Holocene* **22** 773–84

Yao L, Xu Z and Chen X 2019 Sustainable water allocation strategies under various climate scenarios: a case study in China *J. Hydrol.* **574** 529–43

Yuan Y, Shao X, Wei W, Yu S, Gong Y and Trouet V 2007 The potential to reconstruct Manasi River streamflow in the northern Tien Shan Mountains (NW China) *Tree-ring Res.* **63** 81–93

Zawahri N A 2009 India, Pakistan and cooperation along the Indus River system *Water Policy* **11** 1–20

Zhai J, Mondal S K, Fischer T, Wang Y, Su B, Huang J and Uddin J 2020 Future drought characteristics through a multi-model ensemble from CMIP6 over South Asia *Atmos. Res.* **246** 105111

Zhang H 2016 Sino-Indian water disputes: the coming water wars? *Wiley Interdiscip. Rev.: Water* **3** 155–66

Zhang H, He Q, Chen F, Chontoev D, Satylkanov R, Ermenbaev B and Chen Y 2020 August–september runoff variation in the kara darya river determined from juniper (*Juniperus turkestanica*) tree rings in the pamirs-alai mountains, Kyrgyzstan, Back to 1411 CE *Acta Geol. Sin., Engl. Ed.* **94** 682–9